Activity-dependent, homeostatic regulation of neurotransmitter release from auditory nerve fibers

Tenzin Ngodup[a], Jack A. Goetz[a], Brian C. McGuire[b], Wei Sun[c], Amanda M. Lauer[b], and Matthew A. Xu-Friedman[a,1]

[a]Department of Biological Sciences, University at Buffalo, State University of New York, Buffalo, NY 14260; [b]Center for Hearing and Balance and Department of Otolaryngology-Head and Neck Surgery, The Johns Hopkins University, Baltimore, MD 21205; and [c]Center for Hearing and Deafness, Department of Communicative Disorders and Sciences, University at Buffalo, State University of New York, Buffalo, NY 14214

Edited by Gina G. Turrigiano, Brandeis University, Waltham, MA, and approved April 16, 2015 (received for review November 3, 2014)

Information processing in the brain requires reliable synaptic transmission. High reliability at specialized auditory nerve synapses in the cochlear nucleus results from many release sites (*N*), high probability of neurotransmitter release (P_r), and large quantal size (*Q*). However, high P_r also causes auditory nerve synapses to depress strongly when activated at normal rates for a prolonged period, which reduces fidelity. We studied how synapses are influenced by prolonged activity by exposing mice to constant, nondamaging noise and found that auditory nerve synapses changed to facilitating, reflecting low P_r. For mice returned to quiet, synapses recovered to normal depression, suggesting that these changes are a homeostatic response to activity. Two additional properties, *Q* and average excitatory postsynaptic current (EPSC) amplitude, were unaffected by noise rearing, suggesting that the number of release sites (*N*) must increase to compensate for decreased P_r. These changes in *N* and P_r were confirmed physiologically using the integration method. Furthermore, consistent with increased *N*, endbulbs in noise-reared animals had larger VGlut1-positive puncta, larger profiles in electron micrographs, and more release sites per profile. In current-clamp recordings, noise-reared BCs had greater spike fidelity even during high rates of synaptic activity. Thus, auditory nerve synapses regulate excitability through an activity-dependent, homeostatic mechanism, which could have major effects on all downstream processing. Our results also suggest that noise-exposed bushy cells would remain hyperexcitable for a period after returning to normal quiet conditions, which could have perceptual consequences.

homeostasis | release probability | cochlear nucleus

Synapses must be able to transmit information reliably over a range of activity levels. A critical factor in regulating this fidelity is the probability of neurotransmitter release (P_r). If P_r is too high, synapses may have high fidelity at low rates of activity, but they would strongly depress at high rates, which could reduce postsynaptic spiking. If P_r is too low, failure to release neurotransmitter could reduce fidelity.

Activity can influence synaptic properties through multiple mechanisms. One mechanism, homeostatic synaptic scaling, is an activity-dependent regulation of quantal size (*Q*) (1–3), which has recently been reported to occur in vivo (4, 5). One limitation is that changes in *Q* do not change the degree of synaptic depression. Furthermore, increases in *Q* could be limited by receptor number or density. In dissociated hippocampal cell cultures, activity-dependent changes in P_r have been observed (6–8). However, it is not known whether such changes in P_r occur in vivo in the intact brain. In addition, it is not clear how modulation of P_r could prevent depression without also causing large changes in the magnitude of the excitatory postsynaptic current (EPSC).

Fidelity is critical for auditory nerve (AN) synapses onto bushy cells (BCs) in the anteroventral cochlear nucleus (AVCN). AN fibers fire at rates up to 100 Hz spontaneously, and as high as 300 Hz when driven by sound (9–12). At these rates, AN synapses (called endbulbs of Held) show significant depression, which can lead to loss of spiking in BCs (13–18). It is therefore a question how endbulbs transmit information when activity levels are high for extended periods, such as in noisy environments, or in AN fibers with high sensitivity, and whether there are activity-dependent processes that offset depression. Changes in the AVCN and its avian homolog nucleus magnocellularis are observed after such manipulations as extremely intense noise and cochlear or genetic ablation (19–25). However, these manipulations or their effects seem irreversible so it is difficult to assess whether the changes are homeostatic responses to low activity levels.

Here, we show that sound-driven activity regulates P_r in vivo in the auditory pathway at endbulbs. Endbulbs from animals reared in constant noise exhibited less depression and even facilitation. P_r recovered back to high after returning animals to normal sound conditions. We observed no change in *Q*, but rather a compensatory increase in the number of release sites, *N*. Furthermore, BCs from noise-reared animals had higher firing probability during high rates of fiber stimulation. Thus, activity seems to drive homeostatic changes in P_r and *N* at the first stage of the auditory pathway.

Results

Changes in P_r. To assess P_r, we recorded from BCs in whole-cell voltage clamp, isolated individual presynaptic AN fibers, and delivered pairs of stimuli with various intervals. A representative recording is shown in Fig. 1*A*, *Left*, with the endbulb showing typically strong depression at intervals up to 20 ms, reflecting high P_r. From these data, we calculated the paired-pulse ratio (PPR) by normalizing the amplitude of the second EPSC to the first (PPR = $EPSC_2/EPSC_1$) (Fig. 1*B*). PPR was below 1 at all interpulse intervals (Δt) (Fig. 1*B*, open circles). Similar results

NEUROSCIENCE

Significance

Synapses with high probability of neurotransmitter release (P_r) depress during prolonged activity, which reduces the faithful transfer of information. Auditory nerve synapses onto bushy cells show particularly strong depression at physiologically relevant rates of activity, which raises the question of how bushy cells transmit information when sound levels are high for a prolonged period. After rearing mice in constant, nondamaging noise, auditory nerve synapses changed from high to low P_r, with a corresponding increase in the number of release sites, which increased spike fidelity during high activity. Neither quantal size nor average excitatory postsynaptic current changed. After returning to control conditions, P_r recovered to high. These changes seem to reflect a homeostatic response to enhance fidelity.

Author contributions: T.N., W.S., A.M.L., and M.A.X.-F. designed research; T.N., J.A.G., B.C.M., W.S., and A.M.L. performed research; T.N., J.A.G., B.C.M., W.S., A.M.L., and M.A.X.-F. analyzed data; and T.N., A.M.L., and M.A.X.-F. wrote the paper.

The authors declare no conflict of interest.

This article is a PNAS Direct Submission.

[1]To whom correspondence should be addressed. Email: mx@buffalo.edu.

This article contains supporting information online at www.pnas.org/lookup/suppl/doi:10.1073/pnas.1420885112/-/DCSupplemental.

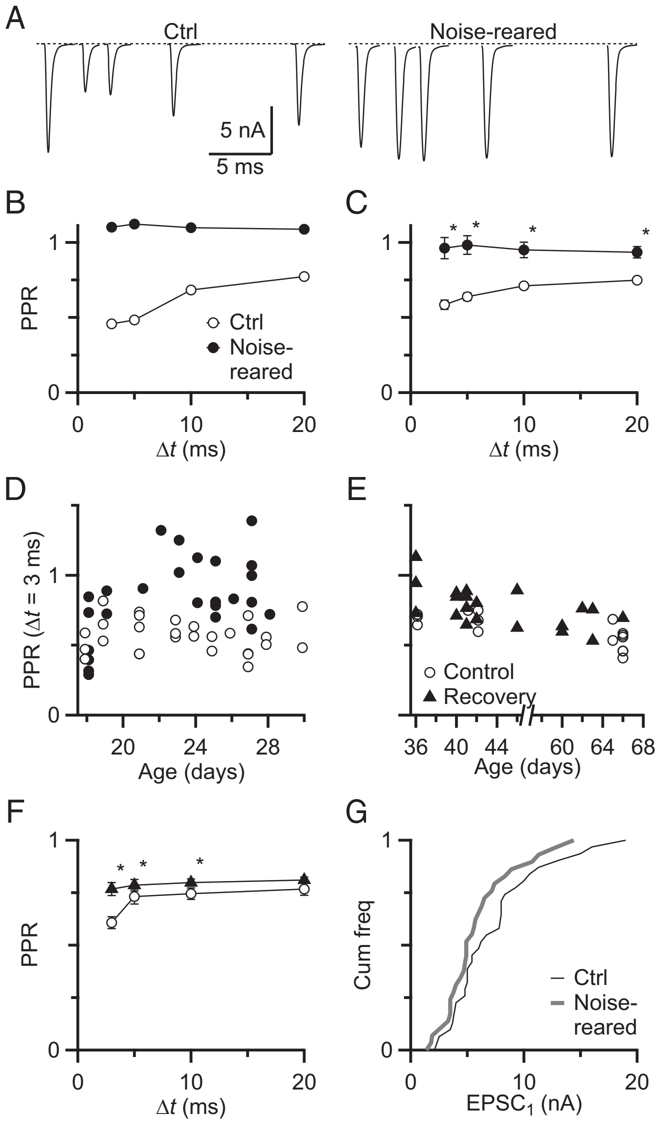

Fig. 1. Noise exposure lowers P_r at the endbulb of Held. AN fibers were stimulated with pairs of pulses of different interpulse intervals, Δt = 3–20 ms. (*A*) Representative traces recorded from P26 BCs from control and noise-reared animals. In control conditions (*Left*), EPSCs show depression at all intervals whereas, after noise rearing (*Right*), EPSCs show no depression, but rather facilitation. (*B*) Paired-pulse ratio (PPR) for the representative experiments in *A*. (*C*) Average PPR for control (n = 17) and noise-reared (n = 22) in animals P21 or older. PPR differed significantly (P < 0.005) at all intervals. (*D*) PPR for control (n = 28) and noise-reared (n = 26) at Δt = 3 ms as a function of age. Noise rearing commenced at P12. (*E*) PPR at Δt = 3 ms for control (open circles) and recovery (closed triangles) BCs. (*F*) Average PPR is slightly elevated over control after recovery (control n = 15; recovery n = 20, P < 0.05 for each interval). (*G*) Cumulative frequency of $EPSC_1$ amplitudes in BCs from control (n = 34) and noise-reared animals (n = 22). The amplitudes do not differ significantly (P > 0.5, Kolmogorov–Smirnov test). Averages in *C* and *F* and in subsequent figures are represented by the mean ± the SEM.

were found in 28 cells in this study (Fig. 1*C*) and are consistent with previous recordings from BCs confirmed by cell filling (14).

We tested the impact of activity on P_r by exposing mice to constant noise beginning at postnatal day 12 (P12) and assessing P_r beginning at P18. The example endbulb in Fig. 1 *A*, *Right* and *B* showed no depression, but rather facilitation for interpulse intervals from 3 to 20 ms. This PPR is well above the range observed under normal conditions. Recordings from a number of BCs showed significant increases in PPR after noise rearing. We confirmed the cell identity using neurobiotin in the intracellular solution in some experiments (control n = 12, noise-reared n = 13) (Fig. S1), and cell structure seemed normal (26–32). PPR for Δt = 3 ms was 0.61 ± 0.04 in control (n = 17) whereas, after noise rearing, PPR was 0.93 ± 0.06 (n = 22), which is significantly higher (P = 0.005, Student's unpaired t test). PPRs at all intervals up to 20 ms were significantly higher (P < 0.05) (Fig. 1 *B* and *C*). The increase in PPR was first observed around P22, during which time PPR is relatively stable in control synapses (Fig. 1*D*). An increase in PPR results from a decrease in P_r so these results suggest that activity plays an important role in setting P_r.

We next tested whether synapses were permanently altered by exposing mice to noise until P26, then allowing recovery in normal sound conditions for at least 2 wk. After restoration of a normal sound environment, the PPR eventually recovered to near normal levels (Fig. 1*E*) although it remained significantly higher than control at all intervals. For Δt = 3 ms, PPR after recovery was 0.767 ± 0.031 (n = 20), which was significantly higher than control BCs (PPR = 0.606 ± 0.028, n = 15, P < 0.05, t test) (Fig. 1*F*). Thus, P_r decreased in noise and increased back near normal levels when normal sound conditions were restored, suggesting that changes in P_r are adaptive and depend on sensory experience.

We tested the effects of noise rearing on general auditory function using auditory brainstem responses (ABRs). There were no significant changes in either threshold or amplitudes of the individual ABR components (Fig. S2). We also assessed hair cell synapses onto auditory nerve afferents by counting CtBP2-immunopositive synaptic ribbons. There was no significant change after noise rearing in the number of ribbons per inner hair cell in base, middle, or apical regions of the basilar membrane (Fig. S3). There were also no noticeable changes in the positions of the synaptic ribbons. Thus, the levels of noise we used for these experiments did not cause any visible, permanent hearing loss or damage to the cochlea.

We also assessed how noise rearing affected the first EPSC ($EPSC_1$) in each pair. There were no significant changes in half-width (control, 0.43 ± 0.01 ms, n = 34; noise-reared, 0.42 ± 0.01 ms, n = 22, P > 0.5) or in decay τ (control, 0.186 ± 0.006 ms, n = 34; noise-reared, 0.174 ± 0.007 ms, n = 22, P > 0.2). These values fit well within the range that we have observed before (14). In addition, the distribution of $EPSC_1$ amplitudes was not significantly changed by noise rearing [P > 0.5, Kolmogorov–Smirnov (K–S) test] (Fig. 1*G*). This lack of change in $EPSC_1$ is surprising because, all else being equal, a decrease in P_r should cause a decrease in $EPSC_1$ amplitude. Therefore, it appears that other factors compensate for the decrease in P_r.

We first considered the quantal size (Q) because it can change homeostatically with activity (1). We recorded miniature EPSCs (mEPSCs) from BCs of control and noise-reared mice. The representative cells in Fig. 2*A* had similar mEPSC frequency (control = 6.4 events per s; noise-reared = 5.3 events per s), similar average mEPSC amplitude (control, 80 pA; noise-reared, 96 pA), and similar distributions of mEPSC amplitude (Fig. 2*B*). On average, noise-reared BCs were not significantly different from control in average mEPSC amplitude (control, 89 ± 5 pA, n = 19; noise-reared, 96 ± 6 pA, n = 12, P = 0.30, K–S test) (Fig. 2*C*) or frequency (control, 3.5 ± 0.32/s, n = 19; noise-reared, 4.8 ± 0.75/s, n = 12, P = 0.37, K–S test) (Fig. 2*D*). Thus, AN synapses did not show obvious homeostatic changes in Q with activity, indicating that another factor must compensate for the decrease in P_r, most likely the number of release sites, N.

To verify quantitative changes in P_r and N, we used the integration method (20, 33–35). Single AN inputs were stimulated with a long train (45 pulses, 100 Hz) (Fig. 2*E*) in the presence of 1 mM kynurenate to prevent AMPA receptor saturation and desensitization. The peak amplitudes of the evoked EPSCs were vs. 9 noise-reared, 10.1 ± 1.0 nA, $P < 0.05$) (Fig. 2*G*, black bars). P_r is calculated by dividing the first EPSC in the train by N. P_r decreased significantly after noise rearing (control, 0.45 ± 0.04 vs. noise-reared, 0.30 ± 0.01, $P < 0.005$) (Fig. 2*G*, white bars). These data reinforce the conclusions based on PPR and $EPSC_1$ data that noise rearing leads to a decrease in P_r and an increase in N.

Anatomical Changes. We considered whether there were changes in synaptic structure consistent with an increase in N. AN synapses are primarily axosomatic (36–38). To quantify such changes, we immunolabeled endbulbs using an antibody against vesicular glutamate transporter-1 (VGLUT-1), which shows strong punctate staining around the BC soma (Fig. 3 *A* and *B*) (30, 38–40). These puncta represent areas of the endbulb containing releasable vesicles, and thus the areas containing release sites. We quantified the average cross-sectional area of puncta in the optical section taken at the midline of each cell. The sizes of puncta around BCs from noise-reared animals were larger than those from controls (control, 1.71 ± 0.18 μm², $n = 10$; noise-reared,

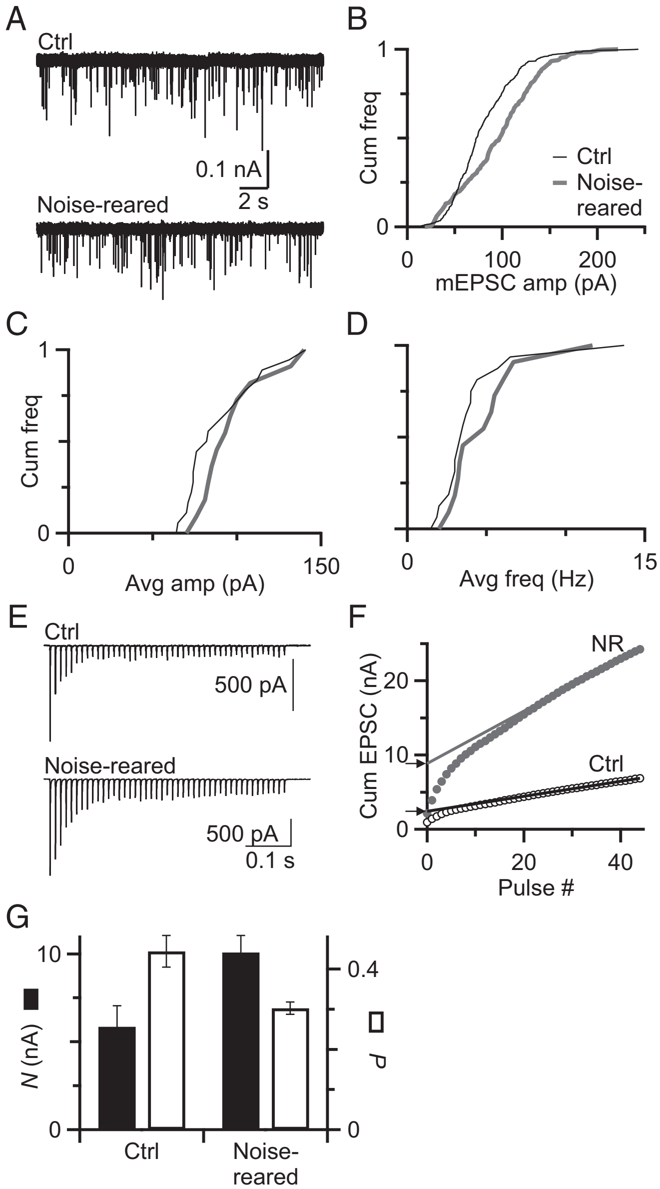

Fig. 2. Noise rearing has no effect on mEPSCs. (*A*) Representative traces showing mEPSCs measured in BCs from control (*Top*) and noise-reared (*Bottom*) animals. (*B*) Cumulative histogram of mEPSC amplitude for the representative cells in *A*. (*C*) Cumulative histogram of average mEPSC amplitudes measured in BCs from control ($n = 19$) and noise-reared ($n = 12$) animals. The distributions do not differ significantly ($P = 0.3$, K–S test). (*D*) Cumulative histogram of mEPSC frequency in BCs from control ($n = 19$) and noise-reared ($n = 12$) animals. The distributions of frequency do not differ significantly ($P = 0.37$). (*E*) Representative EPSC trains recorded in the presence of 1 mM kynurenate from a control and noise-reared BC in response to stimulation of a single presynaptic AN fiber (45 pulses, 100 Hz). (*F*) Derivation of N and P_r from trains data in *E*, using the integration method. EPSC amplitudes are integrated, and a fit is extrapolated back to the *y* axis. Arrowheads mark the estimated value of N. P_r is calculated by dividing the first EPSC by N. (*G*) Average P_r and N measured using the integration method. Noise-reared endbulbs have significantly lower P_r (0.30 ± 0.01, $P < 0.005$) and larger N (10.1 ± 0.1 nA, $P < 0.05$) compared with control ($P_r = 0.45 \pm 0.04$, $N = 5.9 \pm 1.2$ nA).

integrated (markers in Fig. 2*F*), and the steady-state rate of replenishment was estimated by a straight-line fit to the last 20 pulses of the cumulative EPSC (lines in Fig. 2*F*). The *y* intercept of the fit is proportional to N (arrows in Fig. 2*F*), which significantly increased after noise rearing (12 control endbulbs, 5.9 ± 1.2 nA

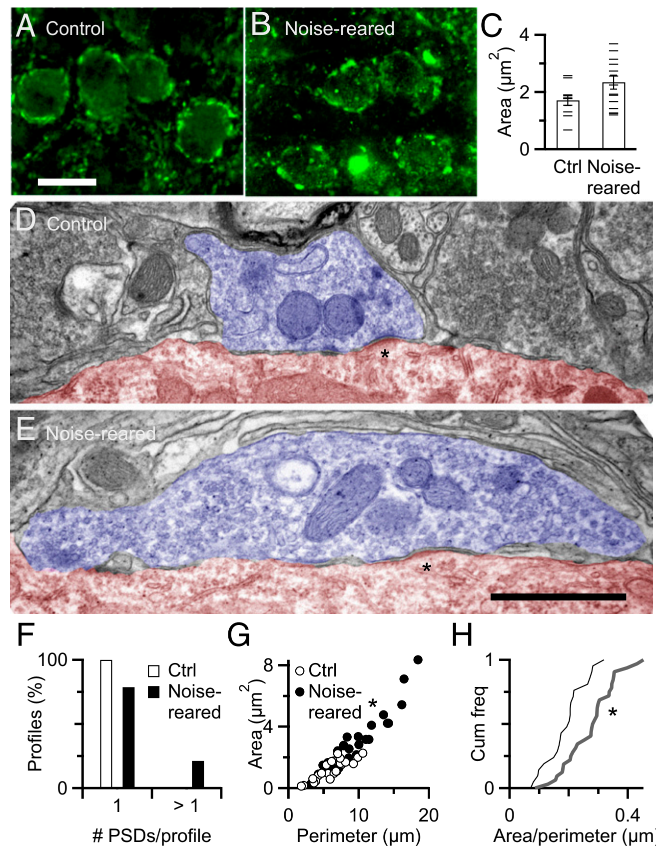

Fig. 3. Anatomical changes at light and ultrastructure levels. (*A* and *B*) Endbulbs immunolabeled for VGLUT-1 in control (*A*) and noise-reared (*B*) animals. BC somata are surrounded by multiple VGLUT-1–positive puncta. (Scale bar: *A* and *B*, 20 μm.) (*C*) Puncta area for endbulbs from control and noise-reared mice. Horizontal lines mark average areas of puncta around individual BCs, and bars are overall averages across all cells (10 control, 15 noise-reared). The average area of puncta around noise-reared BCs is significantly greater than around control BCs ($P < 0.05$). (*D* and *E*) Representative profiles of endbulbs from control (*D*) and noise-reared (*E*) animals. Each profile has numerous synaptic vesicles, curved and asymmetric postsynaptic densities (asterisks). (Scale bar: *D* and *E*, 1 μm.) (*F–H*) Endbulbs in noise-reared mice had significantly more postsynaptic densities per profile ($P < 0.05$, Fisher exact test; *F*), larger profile perimeter and cross-sectional area ($P < 0.001$; *G*) and larger form factors ($P < 0.001$; *H*).

$2.37 \pm 0.25\ \mu m^2$, $n = 15$; $P < 0.05$, *t* test) (Fig. 3*C*). This increase in synaptic area is consistent with an increase in the number of release sites.

To gain a better understanding of the ultrastructural changes underlying the larger area in VGLUT-1 puncta, we examined electron micrographs. AN synapses from control animals resembled those described previously for the CBA/CaJ strain (30). Each section through an endbulb (a "profile") displayed clusters of mitochondria, numerous large round synaptic vesicles, and curved, asymmetric postsynaptic densities (Fig. 3 *D* and *E*). Extended extracellular spaces, mitochondrion adherens complexes, and puncta adherentia were sometimes observed in profiles. Glial sheaths surrounded the synaptic terminals. AN profiles from noise-reared animals seemed generally similar to control.

We quantified differences between quiet- and noise-reared mice ($n = 22$ profiles from control mice, and $n = 33$ profiles from noise-reared mice). Noise-reared mice had more postsynaptic densities (PSDs) per profile ($P < 0.05$, Fisher exact test) (Fig. 3*F*), larger profile cross-sectional areas (control, $1.23 \pm 0.14\ \mu m^2$ vs. noise-reared, $2.59 \pm 0.32\ \mu m^2$, $P < 0.001$, *t* test) (Fig. 3*G*), and larger form factors (area/perimeter, control, 0.19 ± 0.01 µm vs. noise-reared, 0.27 ± 0.02 µm, *t* test, $P < 0.001$) (Fig. 3*H*). Thus, noise-reared endbulbs show clear changes in structure that are consistent with an increase in release site density.

Postsynaptic Effects. Sound-driven activity can influence postsynaptic excitability in other parts of the auditory pathway, such as the medial nucleus of the trapezoid body (41). We examined how noise rearing might influence the intrinsic properties of BCs in the AVCN. Representative responses to depolarizing current injection for control and noise-reared BCs are shown in Fig. 4. Spikes maintained the undershooting amplitude characteristic of BCs (Fig. 4*A*). There were small, but significant, shifts in peak of AP (control, -18.10 ± 2.06 mV, $n = 30$, vs. noise-reared, -22.61 ± 1.38 mV, $n = 32$, $P = 0.03$, *t* test) and threshold voltage (control, -42.49 ± 0.79 mV vs. noise-reared, -45.3 ± 0.77 mV, $P < 0.005$, *t* test) (Fig. 4*B*). Spikes in BCs from noise-reared animals had shorter half-width than control BCs (control, 0.76 ± 0.08 ms, $n = 15$ vs. noise-reared, 0.54 ± 0.05 ms, $n = 26$, $P = 0.03$). We saw no significant difference in the resting membrane potential (control, -56 ± 1 mV; noise-reared, -57 ± 0.5 mV, $P > 0.05$) between control and noise-reared BCs. We also saw no significant change in the input resistance (Fig. S4). The decrease in spike threshold, together with the speeding of the action potential and the decreased synaptic depression, might enhance the likelihood of BCs to respond more reliably during high rates of synaptic activity.

We tested these possibilities directly by doing fiber stimulation in current-clamp recordings. We activated AN fibers using trains of stimuli at different frequencies (100, 200, and 333 Hz). In control conditions, BCs fired reliably early in the trains of stimuli but failed to fire at later pulses, especially for the 333 Hz stimulation rate (Fig. 4*C*, *Left*), presumably because of synaptic depression. However, in noise-reared BCs, spiking was much more reliable for those later pulses (Fig. 4*C*, *Right*). When we quantified spike probability for pulses 11–20, it was much higher for noise-reared BCs at all frequencies tested (K–S test, $P < 0.05$) (Fig. 4*D*). We also quantified spike latency and jitter, but neither was affected significantly by noise rearing ($P > 0.1$) (Fig. S4). Thus, spike reliability increased greatly after noise rearing.

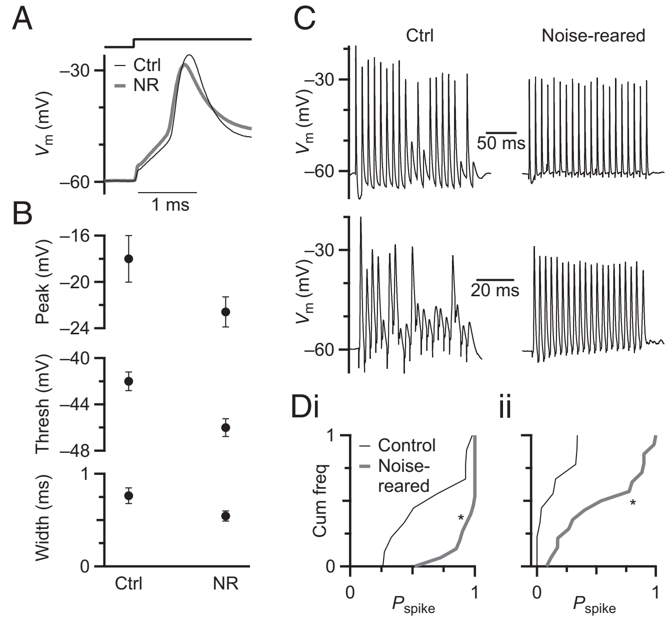

Fig. 4. Effects of noise rearing on spike generation and fidelity of BC spiking. (*A*) Representative current-clamp recordings in response to current pulses of 0.6 nA in control and noise-reared BCs. (*B*) Average measurements of 30 BCs from control and 32 BCs from noise-reared mice, showing significant decreases in action potential peak voltage (*Top*, $P = 0.03$), threshold voltage (*Middle*, $P < 0.005$), and spike half-width (*Bottom*, $P < 0.05$). (*C*) Representative traces showing responses to fiber stimulation at 100 (*Top*) and 333 Hz (*Bottom*) in BCs from control (*Left*) and noise-reared (*Right*) mice. (*D*) Cumulative frequency histogram of spike probability (P_{spike}) over the second half of the stimulation train (pulses 11–20), for experiments similar to *C*. P_{spike} increased significantly after noise rearing ($P < 0.05$, asterisks) for both 100 (*i*) and 333 (*ii*) Hz.

Discussion

We have found that sound-driven activity regulates the endbulb of Held by causing a decrease in P_r and an increase in N. These changes in P_r and N seem to be homeostatic, adaptive responses to noise exposure. The decrease in P_r reduces vesicle depletion during high rates of activity, and N increases to compensate, so that the initial EPSC remains of similar amplitude. We saw no changes in quantal size that would have been consistent with synaptic scaling. Recovery experiments suggest that endbulbs adapt their P_r and N to different sound conditions for at least several weeks after the onset of hearing. These changes seem functionally relevant because noise exposure increased the spiking probability in BCs even during high levels of activity. There could be consequences for auditory processing because the endbulb of Held is a critical gateway for auditory activity entering the brain.

Activity can influence a number of synaptic factors homeostatically. Changes in quantal size, Q, were identified in cultured cells (42, 43) and more recently in vivo (4, 5). In the auditory system, deafferentation or mutations that compromise hearing have been linked to changes in synaptic transmission and postsynaptic excitability (19, 21, 22, 25). In mutants of the synaptic protein Bassoon, auditory nerve activity decreased, endbulb Q and P_r both increased, and N decreased (25). In *dn*/*dn* mutants, which are deaf because of mutations in TMC1 (44), P_r increased, but neither Q nor N changed (21). These results seem largely to complement our observation that increased auditory activity led to decreased P_r and increased N although we observed no evidence of changes in Q, indicating that synaptic scaling may not be a universal mechanism. It is unclear why these changes differ in their details, but one possibility is that genetic manipulation had additional consequences. Excitability can also change through channel expression, phosphorylation, or localization (22, 41, 45). Similar changes likely also take place in BCs in response to noise exposure and could underlie the changes we saw in action potential duration and threshold. Activity in cultured hippocampal cells can also influence P_r (6) although the timescale of this phenomenon seems much faster than that in endbulbs, which retain the decrease in P_r over the course of many hours associated with slice preparation and recording. Furthermore, our findings indicated that the change in P_r in endbulbs was accompanied by a compensatory change in N, and these changes can be recruited in vivo.

It is striking that the average initial EPSC did not change in amplitude even though P_r decreased considerably, indicating not only that N increased to compensate, but also that N increased by just the right amount. Similarly, the average mEPSC rate did not change. This rate is a function of both the number of release sites (i.e., N) and the tendency of each to release, which has been linked to P_r. Thus, these two aspects of synaptic transmission seem to be linked, despite their independent physiological basis. Further experiments will be required to determine whether they are regulated in tandem, or whether changes in one trigger changes in the other through a separate mechanism.

Our experiments reinforce the idea that P_r is not an inconsequential characteristic of synapses. On the contrary, it is tightly regulated so that different synapses show different levels of P_r, even for synapses formed by the same axon (46). Our results further indicate that P_r is regulated depending on the activity level. Even so, P_r can show considerable variability within a single population of synapses, including among auditory nerve fibers (47). The mechanism we have found may help to account for this natural variability: AN fibers with higher activity levels would have lower P_r than those with lower activity. Activity levels in different AN fibers are also highly variable, which correlates with sensitivity to sound (9, 48). We predict that these different classes of AN fiber also have different P_r in the AVCN. Indeed, AN fibers with similar activity levels (i.e., similar intensity sensitivity) seem to converge on the same BC (49). We showed previously that endbulbs that converge on the same BC have similar P_r (50), suggesting that ANs sort onto BCs in a very precise way, presumably to analyze different characteristics of sounds.

The functional consequences of the changes that we observed are dramatic. BCs from noise-reared animals had much higher spiking probability even during high rates of activation. It is interesting to consider possible changes in perception. Decreased P_r could permit sound-driven activity to survive depression at the endbulb, improving perception of sounds even in loud environments. However, when animals return to quiet conditions, activity levels that normally trigger depression and spike failure in quiet-reared animals would cause spikes after noise rearing. Similar increases in excitability have been associated with tinnitus (51–53), and hyperactivity has been seen in inferior colliculus (54), but the cellular origin of this hyperactivity is not clear. Similarly, auditory experience can influence response properties in primary auditory cortex (55–58). Our results indicate that changes as early as the cochlear nucleus also happen and could contribute to the changes seen at higher levels.

It is unlikely that cochlear damage from noise exposure could account for our results. Cochlear damage may not affect ABR threshold, yet can be detected as changes in individual ABR peak amplitudes (59). We saw no changes in ABR threshold, individual ABR peaks, number of ribbons per hair cell, or synaptic ultrastructure after noise treatment. Furthermore, we saw recovery to normal levels of P_r after removing animals from noise. Thus, changes in P_r seem to be specific, adaptive changes in synaptic function in response to elevated levels of activity. Interestingly, we also found that noise exposure increased the spiking probability in BCs even during high levels of activity, which could have strong functional consequences for auditory perception when animals return to quiet conditions.

Materials and Methods

All procedures were approved by the University at Buffalo's Institutional Animal Care and Use Committee. Experiments used CBA/CaJ mice (The Jackson Laboratory) of either sex. Noise exposure was started at P12 (1.6–39 kHz frequency range, 90–94 dB) using a white noise generator (ACO Pacific 3025). Slices of AVCN were prepared at P18–P62, using methods described previously (60). Electrophysiological recordings were made at 34 °C. BCs were identified in voltage clamp by EPSCs with rapid decay kinetics ($\tau <$ 0.2 ms) and half-width $\leq$ 0.5 ms (14), and in current clamp by their undershooting spikes (61). Individual AN fibers were stimulated using a microelectrode placed 30–50 μm away from the soma (A365, WPI). For VGLUT-1 immunohistochemistry, slices containing the AVCN were incubated with primary anti–VGLUT-1 antibodies (1:500; Invitrogen), followed by Texas-red–conjugated goat anti-rabbit secondary (1:200; Jackson ImmunoResearch Laboratories). For electron microscopy, thin sections were cut at 75–100 nm. AN synapses were recognized by characteristic large, round synaptic vesicles, clear cytoplasm, and identifiable postsynaptic densities. Ultrastructural features were measured using ImageJ. See *SI Materials and Methods* for more details.

NEUROSCIENCE

ACKNOWLEDGMENTS. We thank H. Graham for assistance analyzing transmission electron microscopy data, A. Siegel and W. Sigurdson for assistance with confocal images, T. Moser, S. Jung, and D. Ding for advice about CtBP2 immunolabeling, and R. La Rosa, Y. Yang, H. Yang, and X. Zhuang for helpful comments on the manuscript. These experiments were supported by National Institutes of Health (NIH) Grants R03 012352 (to A.M.L.) and R01 DC008125 (to M.A.X.-F.), National Science Foundation Grant 1208131 (to M.A.X.-F.), and the Dalai Lama Trust Fund (T.N.). These experiments were also supported by NIH P30 Grants DC005211 (to the Center for Hearing and Balance) and EY001765 (to the Wilmer Eye Institute Imaging at Johns Hopkins University).

1. Turrigiano GG, Leslie KR, Desai NS, Rutherford LC, Nelson SB (1998) Activity-dependent scaling of quantal amplitude in neocortical neurons. *Nature* 391(6670):892–896.
2. Turrigiano GG, Nelson SB (2004) Homeostatic plasticity in the developing nervous system. *Nat Rev Neurosci* 5(2):97–107.
3. O'Brien RJ, et al. (1998) Activity-dependent modulation of synaptic AMPA receptor accumulation. *Neuron* 21(5):1067–1078.
4. Keck T, et al. (2013) Synaptic scaling and homeostatic plasticity in the mouse visual cortex in vivo. *Neuron* 80(2):327–334.
5. Hengen KB, Lambo ME, Van Hooser SD, Katz DB, Turrigiano GG (2013) Firing rate homeostasis in visual cortex of freely behaving rodents. *Neuron* 80(2):335–342.
6. Branco T, Staras K, Darcy KJ, Goda Y (2008) Local dendritic activity sets release probability at hippocampal synapses. *Neuron* 59(3):475–485.
7. Murthy VN, Schikorski T, Stevens CF, Zhu Y (2001) Inactivity produces increases in neurotransmitter release and synapse size. *Neuron* 32(4):673–682.
8. Zhao C, Dreosti E, Lagnado L (2011) Homeostatic synaptic plasticity through changes in presynaptic calcium influx. *J Neurosci* 31(20):7492–7496.
9. Taberner AM, Liberman MC (2005) Response properties of single auditory nerve fibers in the mouse. *J Neurophysiol* 93(1):557–569.
10. Kiang NY-s (1965) *Discharge Patterns of Single Fibers in the Cat's Auditory Nerve* (MIT Press, Cambridge, MA).
11. Joris PX, Carney LH, Smith PH, Yin TC (1994) Enhancement of neural synchronization in the anteroventral cochlear nucleus. I. Responses to tones at the characteristic frequency. *J Neurophysiol* 71(3):1022–1036.
12. Johnson DH (1980) The relationship between spike rate and synchrony in responses of auditory-nerve fibers to single tones. *J Acoust Soc Am* 68(4):1115–1122.
13. Isaacson JS, Walmsley B (1996) Amplitude and time course of spontaneous and evoked excitatory postsynaptic currents in bushy cells of the anteroventral cochlear nucleus. *J Neurophysiol* 76(3):1566–1571.
14. Chanda S, Xu-Friedman MA (2010) A low-affinity antagonist reveals saturation and desensitization in mature synapses in the auditory brain stem. *J Neurophysiol* 103(4): 1915–1926.
15. Yang H, Xu-Friedman MA (2008) Relative roles of different mechanisms of depression at the mouse endbulb of Held. *J Neurophysiol* 99(5):2510–2521.
16. Cao XJ, Oertel D (2010) Auditory nerve fibers excite targets through synapses that vary in convergence, strength, and short-term plasticity. *J Neurophysiol* 104(5):2308–2320.
17. Wang Y, Manis PB (2008) Short-term synaptic depression and recovery at the mature mammalian endbulb of Held synapse in mice. *J Neurophysiol* 100(3):1255–1264.
18. Kuenzel T, Borst JG, van der Heijden M (2011) Factors controlling the input-output relationship of spherical bushy cells in the gerbil cochlear nucleus. *J Neurosci* 31(11): 4260–4273.
19. Kuba H, Oichi Y, Ohmori H (2010) Presynaptic activity regulates Na(+) channel distribution at the axon initial segment. *Nature* 465(7301):1075–1078.
20. Strenzke N, et al. (2009) Complexin-I is required for high-fidelity transmission at the endbulb of Held auditory synapse. *J Neurosci* 29(25):7991–8004.
21. Oleskevich S, Walmsley B (2002) Synaptic transmission in the auditory brainstem of normal and congenitally deaf mice. *J Physiol* 540(Pt 2):447–455.
22. Lu Y, Monsivais P, Tempel BL, Rubel EW (2004) Activity-dependent regulation of the potassium channel subunits Kv1.1 and Kv3.1. *J Comp Neurol* 470(1):93–106.
23. Takesian AE, Kotak VC, Sharma N, Sanes DH (2013) Hearing loss differentially affects thalamic drive to two cortical interneuron subtypes. *J Neurophysiol* 110(4):999–1008.
24. Jin YM, Godfrey DA, Wang J, Kaltenbach JA (2006) Effects of intense tone exposure on choline acetyltransferase activity in the hamster cochlear nucleus. *Hear Res* 216-217:168–175.
25. Mendoza Schulz A, et al. (2014) Bassoon-disruption slows vesicle replenishment and induces homeostatic plasticity at a CNS synapse. *EMBO J* 33(5):512–527.

26. Wu SH, Oertel D (1984) Intracellular injection with horseradish peroxidase of physiologically characterized stellate and bushy cells in slices of mouse anteroventral cochlear nucleus. *J Neurosci* 4(6):1577–1588.
27. Cao XJ, Shatadal S, Oertel D (2007) Voltage-sensitive conductances of bushy cells of the Mammalian ventral cochlear nucleus. *J Neurophysiol* 97(6):3961–3975.
28. Cant NB, Morest DK (1979) The bushy cells in the anteroventral cochlear nucleus of the cat: A study with the electron microscope. *Neuroscience* 4(12):1925–1945.
29. Cant NB, Morest DK (1979) Organization of the neurons in the anterior division of the anteroventral cochlear nucleus of the cat: Light-microscopic observations. *Neuroscience* 4(12):1909–1923.
30. Lauer AM, Connelly CJ, Graham H, Ryugo DK (2013) Morphological characterization of bushy cells and their inputs in the laboratory mouse (*Mus musculus*) anteroventral cochlear nucleus. *PLoS ONE* 8(8):e73308.
31. Rouiller EM, Ryugo DK (1984) Intracellular marking of physiologically characterized cells in the ventral cochlear nucleus of the cat. *J Comp Neurol* 225(2):167–186.
32. Lorente de Nó R (1981) *The Primary Acoustic Nuclei* (Raven, New York), pp 45–110.
33. Elmqvist D, Quastel DM (1965) A quantitative study of end-plate potentials in isolated human muscle. *J Physiol* 178(3):505–529.
34. Schneggenburger R, Meyer AC, Neher E (1999) Released fraction and total size of a pool of immediately available transmitter quanta at a calyx synapse. *Neuron* 23(2): 399–409.
35. Thanawala MS, Regehr WG (2013) Presynaptic calcium influx controls neurotransmitter release in part by regulating the effective size of the readily releasable pool. *J Neurosci* 33(11):4625–4633.
36. Ryugo DK, Fekete DM (1982) Morphology of primary axosomatic endings in the anteroventral cochlear nucleus of the cat: A study of the endbulbs of Held. *J Comp Neurol* 210(3):239–257.
37. Limb CJ, Ryugo DK (2000) Development of primary axosomatic endings in the anteroventral cochlear nucleus of mice. *J Assoc Res Otolaryngol* 1(2):103–119.
38. Gómez-Nieto R, Rubio ME (2009) A bushy cell network in the rat ventral cochlear nucleus. *J Comp Neurol* 516(4):241–263.
39. Zhou J, Nannapaneni N, Shore S (2007) Vessicular glutamate transporters 1 and 2 are differentially associated with auditory nerve and spinal trigeminal inputs to the cochlear nucleus. *J Comp Neurol* 500(4):777–787.
40. Zeng C, Nannapaneni N, Zhou J, Hughes LF, Shore S (2009) Cochlear damage changes the distribution of vesicular glutamate transporters associated with auditory and nonauditory inputs to the cochlear nucleus. *J Neurosci* 29(13):4210–4217.
41. Song P, et al. (2005) Acoustic environment determines phosphorylation state of the Kv3.1 potassium channel in auditory neurons. *Nat Neurosci* 8(10):1335–1342.
42. Nelson SB, Turrigiano GG (1998) Synaptic depression: A key player in the cortical balancing act. *Nat Neurosci* 1(7):539–541.
43. Thiagarajan TC, Lindskog M, Tsien RW (2005) Adaptation to synaptic inactivity in hippocampal neurons. *Neuron* 47(5):725–737.
44. Kurima K, et al. (2002) Dominant and recessive deafness caused by mutations of a novel gene, TMC1, required for cochlear hair-cell function. *Nat Genet* 30(3):277–284.
45. Grubb MS, Burrone J (2010) Activity-dependent relocation of the axon initial segment fine-tunes neuronal excitability. *Nature* 465(7301):1070–1074.
46. Reyes A, et al. (1998) Target-cell-specific facilitation and depression in neocortical circuits. *Nat Neurosci* 1(4):279–285.
47. Pliss L, Yang H, Xu-Friedman MA (2009) Context-dependent effects of NMDA receptors on precise timing information at the endbulb of Held in the cochlear nucleus. *J Neurophysiol* 102(5):2627–2637.
48. Liberman MC (1978) Auditory-nerve response from cats raised in a low-noise chamber. *J Acoust Soc Am* 63(2):442–455.
49. Ryugo DK, Sento S (1991) Synaptic connections of the auditory nerve in cats: Relationship between endbulbs of Held and spherical bushy cells. *J Comp Neurol* 305(1):35–48.
50. Yang H, Xu-Friedman MA (2012) Emergence of coordinated plasticity in the cochlear nucleus and cerebellum. *J Neurosci* 32(23):7862–7868.
51. Salvi RJ, Wang J, Ding D (2000) Auditory plasticity and hyperactivity following cochlear damage. *Hear Res* 147(1-2):261–274.
52. Manzoor NF, et al. (2012) Noise-induced hyperactivity in the inferior colliculus: Its relationship with hyperactivity in the dorsal cochlear nucleus. *J Neurophysiol* 108(4): 976–988.
53. Mulders WH, Robertson D (2009) Hyperactivity in the auditory midbrain after acoustic trauma: Dependence on cochlear activity. *Neuroscience* 164(2):733–746.
54. Sun W, Deng A, Jayaram A, Gibson B (2012) Noise exposure enhances auditory cortex responses related to hyperacusis behavior. *Brain Res* 1485:108–116.
55. Chang EF, Merzenich MM (2003) Environmental noise retards auditory cortical development. *Science* 300(5618):498–502.
56. Zheng W (2012) Auditory map reorganization and pitch discrimination in adult rats chronically exposed to low-level ambient noise. *Front Syst Neurosci* 6:65.
57. Sanes DH, Bao S (2009) Tuning up the developing auditory CNS. *Curr Opin Neurobiol* 19(2):188–199.
58. Popescu MV, Polley DB (2010) Monaural deprivation disrupts development of binaural selectivity in auditory midbrain and cortex. *Neuron* 65(5):718–731.
59. Kujawa SG, Liberman MC (2009) Adding insult to injury: Cochlear nerve degeneration after "temporary" noise-induced hearing loss. *J Neurosci* 29(45):14077–14085.
60. Yang H, Xu-Friedman MA (2010) Developmental mechanisms for suppressing the effects of delayed release at the endbulb of Held. *J Neurosci* 30(34):11466–11475.
61. Oertel D (1983) Synaptic responses and electrical properties of cells in brain slices of the mouse anteroventral cochlear nucleus. *J Neurosci* 3(10):2043–2053.